scientific reports

Check for updates

OPEN

Age, not growth, explains larger body size of Pacific cod larvae during recent marine heatwaves

Jessica A. Miller[1]✉, L. Zoe Almeida[1,4], Lauren A. Rogers[2], Hillary L. Thalmann[1], Rebecca M. Forney[1] & Benjamin J. Laurel[3]

Marine heatwaves (MHWs) are often associated with physiological changes throughout biological communities but can also result in biomass declines that correspond with shifts in phenology. We examined the response of larval Pacific cod (*Gadus macrocephalus*) to MHWs in the Gulf of Alaska across seven years to evaluate the effects of MHWs on hatch phenology, size-at-age, and daily growth and identify potential regulatory mechanisms. Hatch dates were, on average, 19 days earlier since the onset of MHWs, shifting a mean of 15 days earlier per 1 ℃ increase. Size-at-capture was larger during & between MHWs but, contrary to expectations, larvae grew slower and were smaller in size-at-age. The larger size during & between MHWs can be entirely explained by older ages due to earlier hatching. Daily growth variation was well-explained by an interaction among age, temperature, and hatch date. Under cool conditions, early growth was fastest for the latest hatchers. However, this variation converged at warmer temperatures, due to faster growth of earlier hatchers. Stage-specific growth did not vary with temperature, remaining relatively similar from 4 to 8 ℃. Temperature-related demographic changes were more predictable based on phenological shifts rather than changes in growth, which could affect population productivity after MHWs.

Keywords Temperature Size Rule (TSR), Otolith growth

Prolonged periods of extreme temperatures in the ocean, or marine heatwaves (MHWs), appear to be increasing in frequency, duration, and intensity around the world[1,2], but these patterns could be explained by longer-term warming trends[3]. MHWs are stressful for marine and human communities and can have widespread ecological[4] and socio-economic impacts[5]. However, MHWs also provide an opportunity to evaluate mechanistic hypotheses about how individuals respond to warming in natural environments. During the latter part of 2014 through 2016, the northeast Pacific Ocean experienced an extreme, prolonged MHW, which was followed by another substantial heatwave in 2019[6]. The 2014–2016 heatwave in the Gulf of Alaska (GOA) is the longest MHW on record (> 700 days)[7] and impacted the ecosystem for years by way of low productivity[6], mass mortality events, and reduced fisheries resources[8–10], including a 75% decline in Pacific cod (*Gadus macrocephalus*) biomass and subsequent closure of the fishery in 2020. There was also an extended period of poor recruitment during the MHWs, which delayed the recovery of the cod stock[11]. In this study, we focused on larval Pacific cod to determine how individual age, size, and growth responded to MHWs throughout their first year of life across multiple years.

Warming oceans have been associated with declines in productivity and abundance[12] and can lead to increases in mortality rates[13]. For example, the abundance of Pacific cod has consistently been greater during cooler periods[14,15]. However, the mechanisms underlying this pattern remain unclear. Temperature can influence the time of hatch as well as hatch success. For Pacific cod, there is evidence for a relatively narrow thermal window (~ 4 to 6 ℃) for embryonic development and hatch success[16,17]. Additionally, in the GOA, larval[18] and juvenile[19,20] Pacific cod collected in standardized surveys are larger at capture during warmer years, which could be due to earlier spawn timing and older ages, faster growth, enhanced selective mortality, or a combination of these factors.

[1]Department of Fisheries, Wildlife, and Conservation Sciences, Coastal Oregon Marine Experiment Station, Hatfield Marine Science Center, Oregon State University, 2030 SE Marine Science Drive, Newport, OR 97365, USA. [2]Recruitment Processes Program, Resource Assessment and Conservation Engineering Division, Alaska Fisheries Science Center, National Marine Fisheries Service, NOAA, Seattle, WA, USA. [3]Fisheries Behavioral Ecology Program, Resource Assessment and Conservation Engineering Division, Alaska Fisheries Science Center, Hatfield Marine Science Center, National Marine Fisheries Service, NOAA, Newport, OR 97365, USA. [4]Present address: Cornell Biological Field Station, Department of Natural Resources and the Environment, Cornell University, 900 Shackelton Point Road, Bridgeport, NY 13030, USA. ✉email: Jessica.Miller@oregonstate.edu

However, catch rates of larvae and juveniles are also lower during warmer years and were at their lowest during the MHWs, which could be related to reduced spawning effort or hatch success, differential spatial distribution, increased mortality, or a combination of factors[8,20]. Variation in other environmental factors, such as timing of seasonal stratification and strength of alongshore transport, which can influence the production of mesoscale eddies that can affect productivity and larval retention in shelf waters, and predator and prey composition, can affect growth and survival and is often correlated with temperature, further complicating efforts to identify causative factors for population declines[21]. The uncertainty regarding the processes behind poor recruitment and reduced productivity associated with MHWs highlights the need for greater mechanistic understanding of the relationship between climate and recruitment, particularly as extreme climate events become more common[2,3,22].

Warming can affect marine populations in many ways, including shifts in reproductive phenology or spatial distribution, with movement poleward or to deeper, cooler waters[23]. However, there are limits to how far individuals can move to avoid unfavorable temperatures. For example, poleward movement in the northern GOA is limited by the Alaska Peninsula, which requires fish to travel westward to pass through Unimak Pass, the only major passage to the eastern Bering Sea[24]. Therefore, understanding how phenotypic and genetic variation allows individuals to respond and adapt will be key to understanding and predicting consequences of short- and long-term warming.

A widespread observation for both aquatic and terrestrial species is the reduction in age- and size-at-maturity as temperatures warm, a phenomenon referred to as the temperature-size rule (TSR)[25,26]. Faster early growth at warmer temperatures, leading to earlier maturity at smaller body size, is often invoked as a mechanism behind the TSR. However, for age-0 Pacific cod juveniles collected during the summer in GOA coastal nurseries[20], the larger body size observed during recent MHWs could not be explained by faster growth alone. Rather a combination of shifts in phenology, leading to earlier hatch dates and older juveniles, combined with relatively small increases in growth rate after ~ 75 days post hatch (dph) and, potentially, enhanced size-selective mortality[27] contributed to those larger body sizes. Therefore, basic relationships, such as temperature-dependent growth models, are unlikely to predict novel demographic changes emerging under climate change.

We expand upon research on post-settlement, age-0 juvenile Pacific cod[20,27] that were collected during summer by focusing on an earlier life stage, pre-settlement larvae, collected in the spring from 2006 to 2019. We examined archived larval collections to (1) determine the hatch phenology; (2) estimate daily size-at-age and early growth histories; and (3) evaluate physical and biological factors that are potentially related to variation in hatch timing, daily growth, and size-at-age. Our reconstructed age and growth histories allow us to determine if shifts in body size during the early life history that were observed during MHWs are better explained by shifts in phenology or growth.

Results

To compare hatch phenology, size, and growth before and during & between MHWs, we grouped larvae collected in the northern GOA (Fig. 1) according to MHW status. MHWs were defined as anomalous events during which temperatures were warmer than the 90th percentile of the 30 year baseline period of 1983–2012 for five days or more[28,29]. We had one year, 2017, that was relatively warm compared to earlier years but not classified as a heatwave event (Fig. 2). Therefore, we included 2017 in the "during & between" group, along with the MHW years 2015 and 2019. The years 2006, 2009, 2010, and 2013 were included in the "before" MHW group.

Age, hatch date, and incubation duration

Since 2015, Pacific cod larvae have been longer (mean = 10.8 ± 3.21 SD versus 8.3 ± 2.44 SD mm total length, TL) and older (32.4 dph ± 2.7 SD versus 19.5 dph ± 5.1 SD) at capture with earlier mean hatch dates (17 April versus 6 May) (Table 1). The earliest mean annual hatch date occurred in 2019 (11 April) and the latest occurred over a month later (17 May) in 2009. Pairwise differences in mean annual hatch date before and during & between MHWs ranged from 5 (2015 compared with 2006) to 36 days earlier (2019 versus 2009).

We compared hatch dates before and during & between MHWs (Fig. 3) with a linear mixed model (LMM). A model with collection year and survey station as random effects performed slightly better than models with only one or neither factor (AIC = 16,046 with both random effects versus > 16,128 for other models). There was a slight negative skew in model residuals due to 13 fish with hatch dates earlier than 21 March in 2006, 2009, and 2017. However, given that large sample sizes ($n = 2262$) are relatively robust to departures from normality, these larvae were not removed (and results were qualitatively the same either way). The final LMM to predict hatch date with MHW status as a fixed effect and year and station as random factors explained a little over half the variation in hatch dates. The model's explanatory power related to the fixed effects alone (marginal R^2) was 0.160 and the total R^2 was 0.613. The model's intercept, corresponding to the mean hatch date (day of year) before MHWs was 125.30 (95% CI 118.17 to 132.43, $t_{2257} = 34.48$, $P < 0.001$) (Supplementary Table S1). The effect of MHWs indicated that hatch dates occurred an estimated 19 days earlier during & between MHWs than before (beta = −18.54 (95% CI −29.53, −7.54, $t_1 = -3.31$, $P < 0.001$).

Mean temperature at 100 to 250 m depth during the spawning period (January to April, "$T_{J\text{-}A,\ 100–250\ m}$") ranged from 4.93 ℃ in 2009 to 6.89 ℃ in 2019 (Supplementary Table S2). We also estimated an annual mean incubation duration by determining the number of days immediately prior to a fish's hatch date needed to reach a cumulative degree day of 110 ℃ based on GAK1 temperatures at 100 to 250 m depth. Cumulative degree days (CDD) provide an estimate of thermal exposure, are often used to quantify developmental rates in agronomy and aquaculture[30], and can be used to examine variation in size and growth in ectotherms[31] (see Methods for additional detail).

Annual mean temperature during embryonic incubation periods was highly correlated with $T_{J\text{-}A,\ 100–250\ m}$ ($r = 0.944$, $n = 7$, $P = 0.006$), but incubation temperatures were a bit cooler than $T_{J\text{-}A,\ 100–250\ m}$, ranging from 4.57 ℃ in 2009 to 6.64 ℃ in 2019 (Supplementary Table S2). Estimates of incubation duration ranged from 17 days in

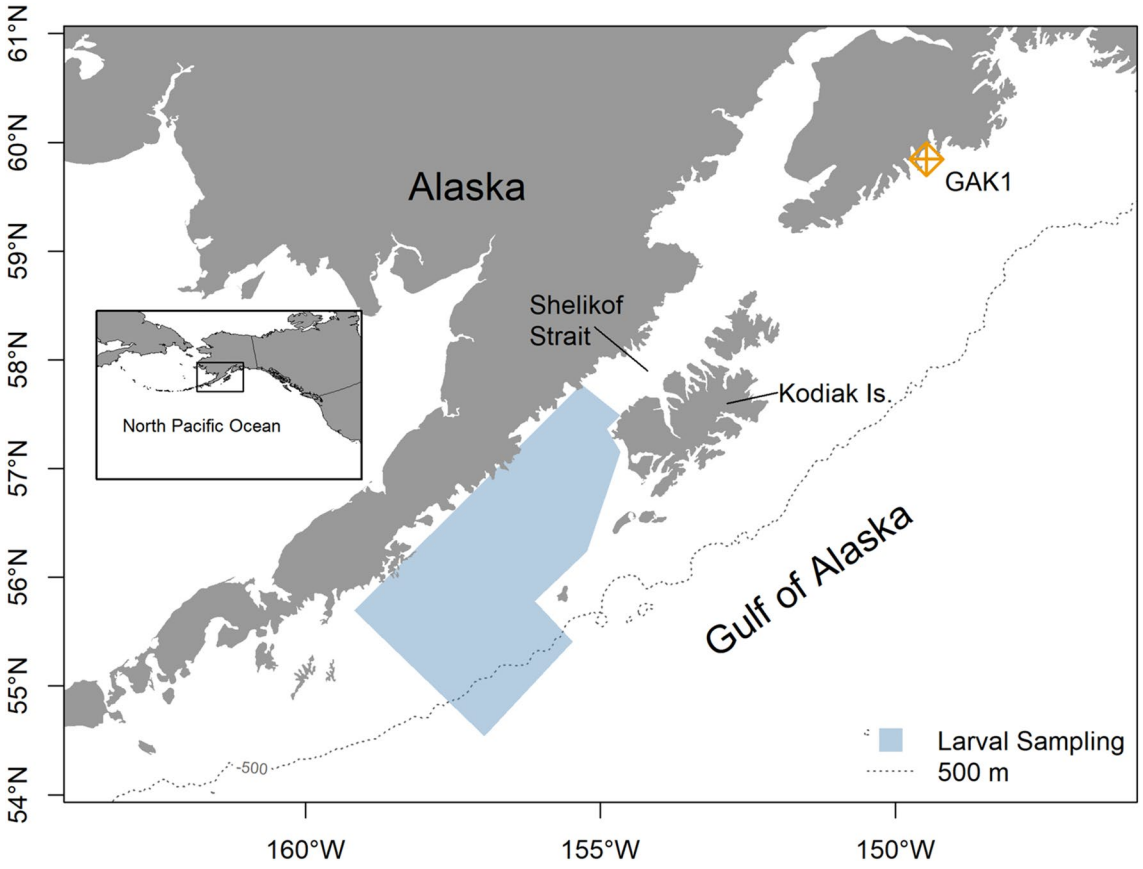

Figure 1. Location of survey area for collection of Pacific Cod larvae (blue polygon). The location of the hydrographic station (GAK1) is also indicated.

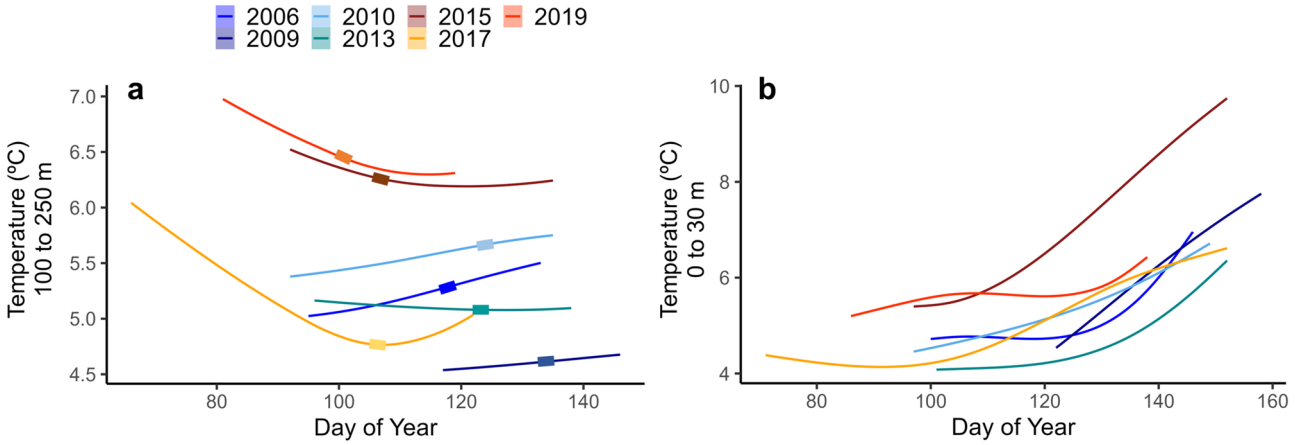

Figure 2. Daily temperature experienced by larvae from first day of hatching to last day of capture in years before (2006, 2009, 2010, 2013) and during & between (2015, 2017, 2019) marine heatwaves. Mean temperature from (**a**) 100 to 250 m was used for initial 5 days of life and (**b**) surface to 30 m for 6 days post hatch to capture. Colored boxes in (**a**) indicate mean hatch date for each year. Temperature data are from the GAK1 hydrological station.

2019 to 24 days in 2009 (Table 1). Based on pairwise comparisons between years, differences in mean temperature during incubation, or the direct effects of temperature on embryonic development rate, could account for 1 (2009 versus 2017) to 7 days (2009 versus 2019) of the observed differences in mean hatch date. However, the pairwise differences in observed hatch dates before and during & between MHWs ranged from 5 to 36 days. Therefore, estimated shifts in incubation duration could only account for ~ 20% of the largest difference in mean

Year	MHW	Earliest HD	Latest HD	Mean HD	Incub. Dur. (d)	Cap. date	TL (mm)	Age (dph)	Daily growth (mm/day)	Larval CPUE	*n*, all	*n*, otolith
2006	Before	19 Mar	18 May	28 Apr	21	24 May	9.7 (2.4)	26.0 (9.0)	0.38 (0.04)	11.96	627	22
2009	Before	25 Apr	28 May	17 May	24	31 May	7.2 (1.8)	13.7 (6.4)	0.58 (0.13)	14.59	372	48
2010	Before	14 Mar	23 May	06 May	20	26 May	8.5 (2.5)	20.0 (13.0)	0.53 (0.22)	3.17	120	21
2013	Before	29 Mar	23 May	04 May	22	23 May	7.8 (2.3)	18.4 (9.6)	0.47 (0.10)	55.66	961	47 (44)
2015	During/ Between	01 Mar	15 May	23 Apr	18	26 May	11.1 (3.8)	32.8 (19.0)	0.41 (0.14)	0.37	21	10
2017	During/ Between	01 Mar	09 May	17 Apr	23	22 May	10.9 (3.2)	34.9 (14.2)	0.32 (0.04)	4.94	147	37 (34)
2019	During/ Between	21 Mar	24 Apr	11 Apr	17	11 May	9.5 (2.5)	29.6 (9.7)	0.34 (0.08)	0.45	14	14

Table 1. Metrics associated with larval Pacific cod collections, including year of capture (Year), marine heatwave status (MHW), earliest, latest, and mean hatch date (HD), estimated incubation duration (Incub. Dur. in days), mean capture date (Cap. date), and mean (SD) for total length (TL, mm) at capture, age (days post hatch, dph), absolute daily growth rate (TL/age = mm/day), catch per unit effort (CPUE, no. per 10 m^2). Sample sizes for all larvae with length measurements (*n*, all) and for the larvae included in otolith-based age analyses (*n*, otolith) and those included in the otolith-based growth analyses in parentheses.

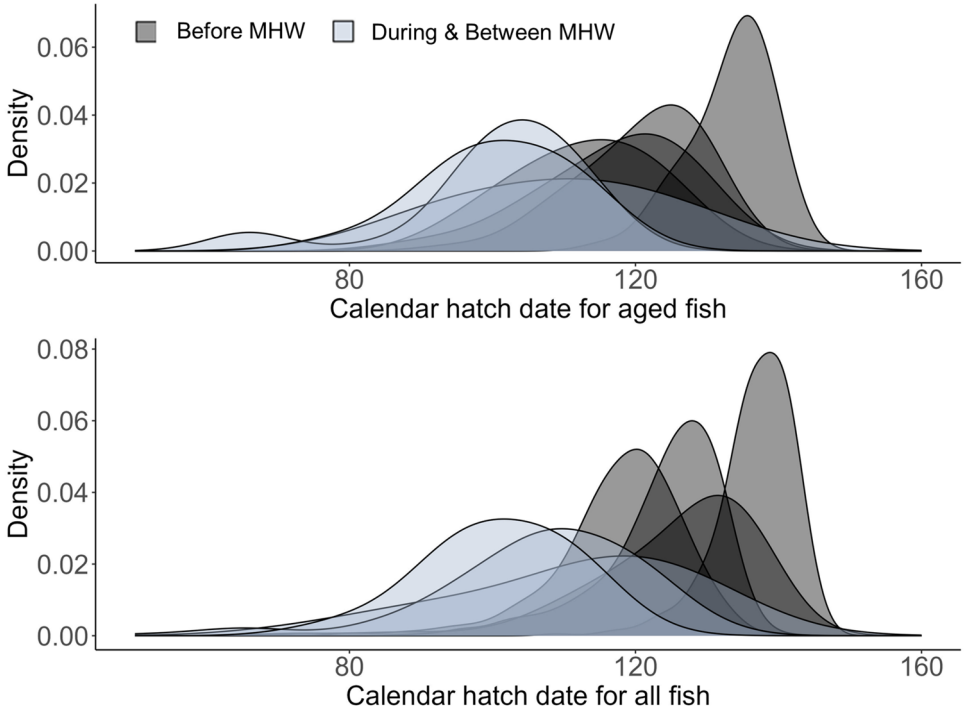

Figure 3. Hatch date density distributions before (2006, 2009, 2010, 2013) and during & between (2015, 2017, 2019) the marine heatwaves (MHWs) for larvae that were aged based on otolith analysis ($n = 201$, top graph) and all larvae ($n = 2262$), bottom graph).

hatch dates (7 of 36 days), indicating other factors, such as changes in parental spawning behavior or increased selective mortality, contributed to the shifts in hatch dates during & between the MHWs.

Mean annual hatch dates were negatively associated with water temperature (Fig. 4). A linear model with deep temperatures during the spawning period ($T_{J\text{-}A,\ 100\text{–}250\ m}$) was more parsimonious than a model with incubation temperatures (AIC = 50.4 versus 55.0, respectively). The final model (mean hatch date = 204.10 (± 23.11 SD) – 14.68 (± 3.91 SD) · $T_{J\text{-}A,\ 100\text{-}250\ m}$, $F_{1,5} = 14.10$, $P = 0.013$, $R^2_{adj} = 0.686$) indicated that, from 2006 to 2019, hatch dates shifted a mean of 14.7 days earlier for each degree of warming during January through April (Supplementary Table S3).

Size-at-age

We compared larval size-at-age before and during & between MHWs with a LMM. This LMM was limited to individuals > 4.79 mm TL and < 17 mm TL and < 51 dph ($n = 2162$ larvae) due to few very small (< 5 mm TL),

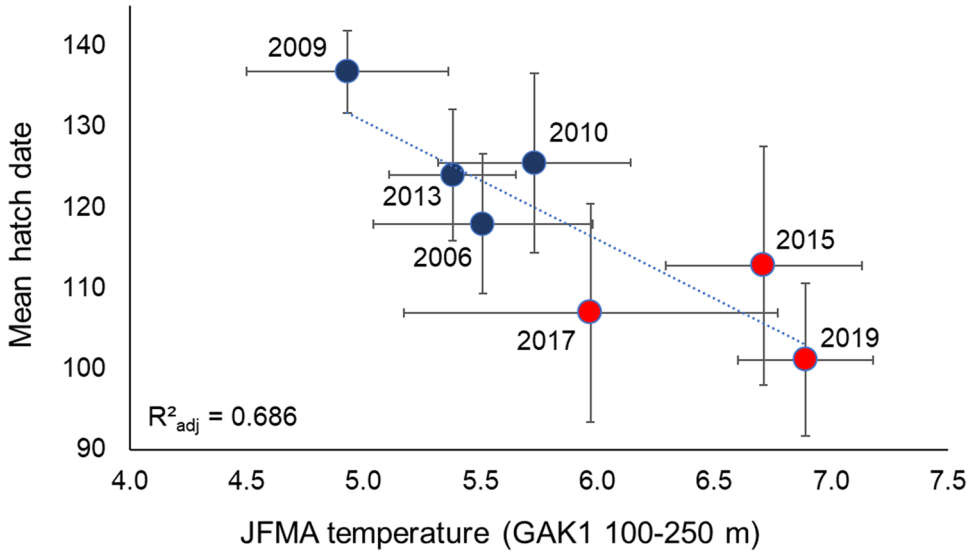

Figure 4. Predicted mean (± SD) hatch date and water temperatures from January through April (JFMA) at 100 to 250 m depth. Data for larvae collected before (2006, 2009, 2010, 2013; blue circles) and during & between (2015, 2017, 2019; red circles) the marine heatwaves are included. Temperature data are from the GAK1 hydrological station.

large (> 17 mm TL), or old (> = 51 dph) larvae. Length was square root transformed to meet model assumptions and the inclusion of year as a random factor improved the model (AIC = 3006 for year versus 3469 without). However, the models with only year as a random effect and with year and station as random effects were similar (AIC difference was < 2). Therefore, the final model, estimated using restricted maximum likelihood (REML) and an nlminb optimizer, included a second-degree polynomial fit for age and MHW status as fixed effects and year as a random effect (Supplementary Table S4; Fig. 5). Standardized parameters were obtained by standardizing the covariates to aid in model interpretation, i.e., age was scaled by subtracting the mean and dividing by the standard deviation. The model's total explanatory power was high (conditional $R^2 = 0.960$), largely driven by fixed effects alone (marginal $R^2 = 0.920$). The model's intercept (8.66) corresponds to length at scaled age = 0 (~ 20 dph) before the MHWs (Supplementary Table S4). There were interactions between age and MHW status, with size-at-age larger before MHWs (Fig. 3). This pattern was reflected in the model's marginal means, with TL being 1.9% and 10.9% longer at ~ 6 and 25 dph, respectively, before the MHWs (Supplementary Table S5).

Daily growth

We compared daily relative growth before and during & between MHWs using a LMM. For this LMM, age was limited to larvae < 67 dph ($n = 193$ larvae with 4820 daily growth increments) due to issues with model convergence when the three larvae > 80 dph were included. We used relative growth rates rather than absolute growth rates to account for variation in size across years and MHW status. We compared models with all potential

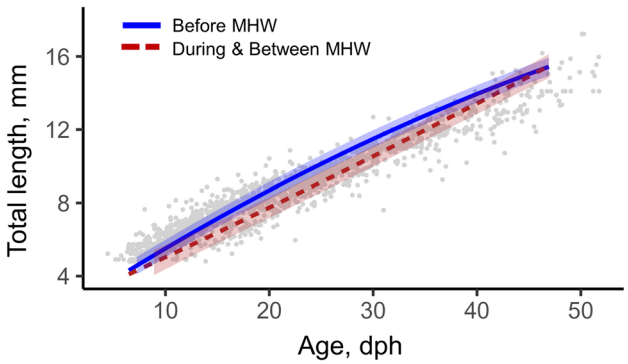

Figure 5. Size-at-age: total length at capture (mm) by age (days post hatch, dph) for larvae collected before (2006, 2009, 2010, 2013) and during & between (2015, 2017, 2019) the marine heatwaves (MHWs). Model predictions (lines) are included for years before and during & between the MHWs. Grey points are observed data.

predictor variables (scaled age, scaled temperature, scaled hatch date) and all interactions with or without day of life for each fish as a random effect, and the model with the random effect was supported (AIC = −34,358 with the random effect versus -32,276 without). All potential predictor variables contributed to the model and there was a significant three-way interaction among scaled age, scaled temperature, scaled hatch date. Therefore, all variables and their interactions remained in the models for comparison with or without a first order auto-regressive parameter. The most parsimonious model also included a first order auto-regressive parameter (AIC = −34,827 with versus −34,181 without).

The final model's explanatory power was high (conditional $R^2 = 0.701$) with the fixed effects accounting for 47% of the variation (marginal $R^2 = 0.469$). The model's intercept (0.028) corresponds to relative growth (mm/mm/day) at scaled age = 0 (~ 13 dph), scaled temperature = 0 (5.5 ℃) and scaled hatch date = 0 (April 20) (Table 2). There were interactions between and among all variables and a three-way interaction among scaled age, scaled temperature, and scaled hatch date. Given the three-way interaction indicates that one, or more, of the interactions differ across levels of the third factor, we visualized the patterns by plotting the marginal mean relative daily growth at age for early (April 8), mid (April 20), and late (May 6) hatch dates at temperatures of 4.5, 5.5, and 6.5 ℃ (Fig. 6, lines) along with observed growth (Fig. 6, grey points).

Growth declined with age, as expected, although the rate of decline varied with temperature and hatch date. At cooler temperatures and younger ages, the fastest growth was associated with later hatch dates, which also experienced the most rapid decline in growth with age (Fig. 6, left panel). However, the growth benefit early in life associated with later hatching was reduced at intermediate temperatures (Fig. 6, middle panel) and essentially gone at warmer temperatures (Fig. 6, right panel), and the change was due primarily to relatively faster growth rates at the youngest ages (< 15 d) for earlier hatchers rather than declines in growth of the later hatchers. The

Term	Value (SE)	*t*-value	p-value
Intercept	0.0279 (0.0004)	69.50	< 0.0001
Scaled Age	−0.0098 (0.0004)	−24.23	< 0.0001
Scaled Temp	0.0018 (0.0002)	6.21	< 0.0001
Scaled HD	−0.0008 (0.0004)	−2.11	0.0363
Scaled Age:Scaled Temp	0.0005 (0.0002)	2.18	0.0294
Scaled Age: Scaled HD	−0.0040 (0.0004)	−10.52	< 0.0001
Scaled Temp:Scaled HD	−0.0008 (0.0002)	−3.15	< 0.0001
Scaled Age: Scaled Temp:Scaled HD	0.0014 (0.0002)	7.20	< 0.0001

Table 2. Results from models to predict daily relative growth (mm/mm/day) based on age, temperature, and hatch date. Model terms and their value (SE = standard error) are included with t-value, and p-value. Data were scaled for analysis.

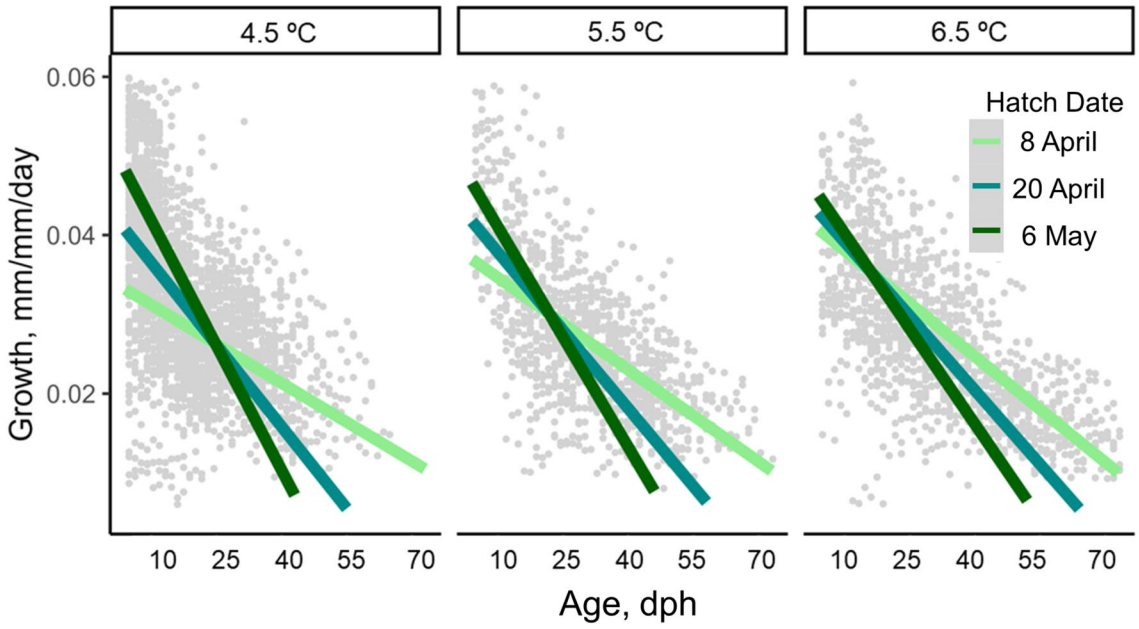

Figure 6. Predicted marginal mean relative growth (mm/mm/day) from linear mixed model holding temperature at 4.5 °C, 5.5 °C, or 6.5 °C and hatch dates at 8 April, 20 April, or 6 May. Data observations are indicated by grey circles, and 85% of the data fall within this temperature range.

interaction was due to a convergence of growth rates across hatch times in warmer waters. Later in life, after ~ 30 dph, the earlier hatchers consistently had faster growth rates.

We visualized observed relative growth before and during & between MHWs by binning all data into three groups for temperature (< 5.0 ℃, between 5.0 and 5.7 ℃ and > 5.7 ℃) and for hatch date ("Early" = 6 March to 15 April, "Middle" = 16 April to 27 April, and "Late" = 28 April to 21 May), with each bin including ~ 33% of the observations, which highlighted several points (Fig. 7). First, during & between MHWs, the late hatchers (28 April to 21 May) were only present at the warmest temperatures (> 5.7 °C). Second, within a MHW status, growth rates declined as temperatures warmed. Third, within a temperature range, growth rates were always faster for later hatchers regardless of MHW status. Fourth, the decline in growth with age was reduced or disappeared for the earliest hatchers (6 March to 15 April) at the warmest (> 5.7 ℃) temperatures before the MHWs and at all temperatures during & between the MHWs (Fig. 7, blue lines).

We also compared growth rates across temperature for fish of comparable age early (6 to 20 dph) and later (31 to 45 dph) in their larval life by hatch date ("Early", "Middle", and "Late", as defined above) before and during & between the MHWs. This comparison highlights how consistent growth was across temperatures (Fig. 8a,b). Growth rates were, expectedly, faster earlier in life (6 to 20 dph) than later in life (31 to 45 dph). However, growth rates before and during & between MHWs mostly overlapped for both periods although the warmest temperatures (> 8 ℃) were rarely experienced before 2015 and only by middle and late hatchers (Fig. 8a,b).

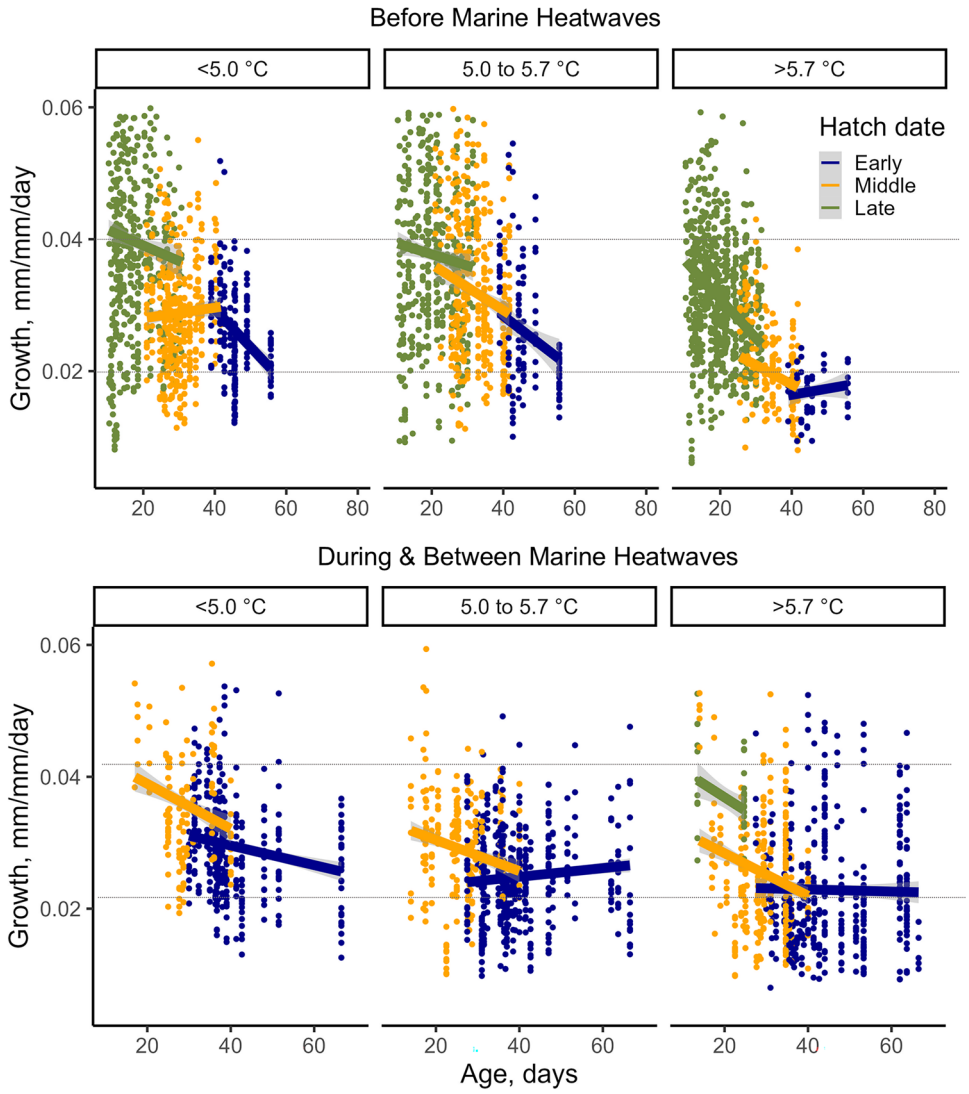

Figure 7. Observed relative growth (mm/mm/day) for larvae with variable hatch dates across the temperature range (colored points) and predictions (colored lines) from the linear mixed model that included temperature, hatch date, and age. "Early" indicates hatch dates from 6 March to 15 April, "Middle" from 16 to 27 April, and "Late" from 28 April to 21 May. Data are separated by marine heatwave (MHW) status for visualization although MHW status was not included in the model due to collinearity issues. Dotted lines at 0.04 and 0.02 mm/mm/day are for reference.

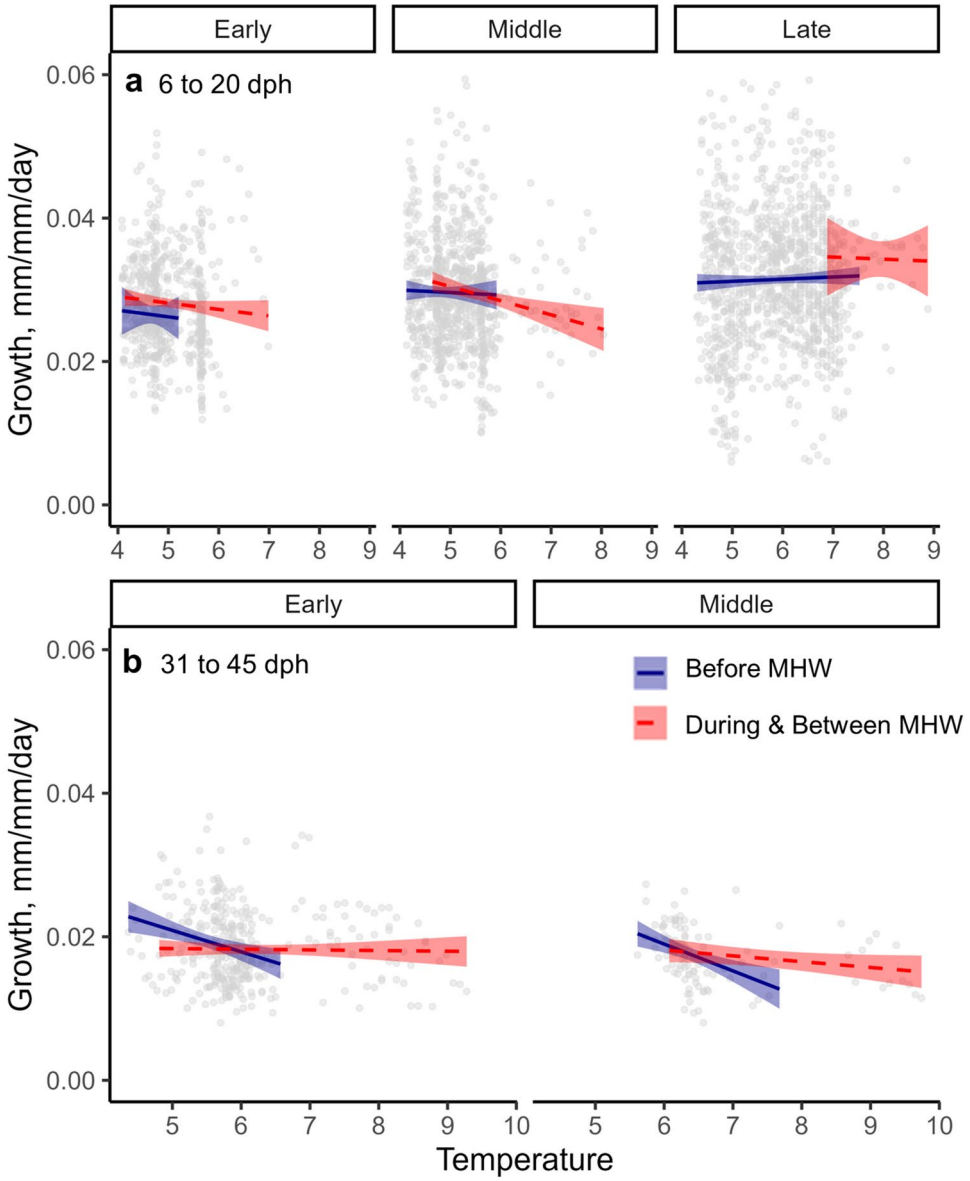

Figure 8. Observed relative growth (mm/mm/day) for larvae with variable hatch dates before and during & between marine heatwaves (MHWs). "Early" indicates hatch dates from 6 March to 15 April, "Middle" from 16 to 27 April, and "Late" from 28 April to 21 May. (**a**) Growth for larvae from 6 to 20 dph and (**b**) from 31 to 45 dph are presented. Lines represent predictions from the linear mixed model. Years before heatwaves (2006, 2009, 2010, 2013) are solid, blue line and years during & between heatwaves (2015, 2017, 2019) are dashed, red line. Linear fits with 95% confidence intervals are presented.

Lifetime thermal history using Cumulative Degree Day (CDD)

We summed the daily mean temperature experienced on each day of life for each larvae to generate a mean daily estimate of CDD for each year. The comparison of interannual variation in CDD in relation to age (dph) (Fig. 9) demonstrates that the lifetime thermal histories were similar across years until approximately 25 dph. From 25 to 50 dph, larvae collected in 2015, which was the first full year of the recent MHWs, experienced the greatest CDD at age (Fig. 9). Additionally, from 30 to 45 dph, larvae collected in 2013 experienced the lowest CDD. Otherwise, CDD experienced at age was similar across years.

Relationships with annual phytoplankton bloom

Pacific cod larvae (< 7 mm TL) primarily feed initially on copepod nauplii and then consume various copepodites and adult copepods as well as eggs as they grow[32]. In the GOA, secondary production follows the spring phytoplankton bloom and can provide a relative indication of interannual variation in productivity[21]. Therefore, we compared annual mean hatch phenology and absolute growth rates (mm/day) with annual estimates of the timing of bloom initiation in the GOA. Hatch dates were positively, but not significantly, associated with bloom

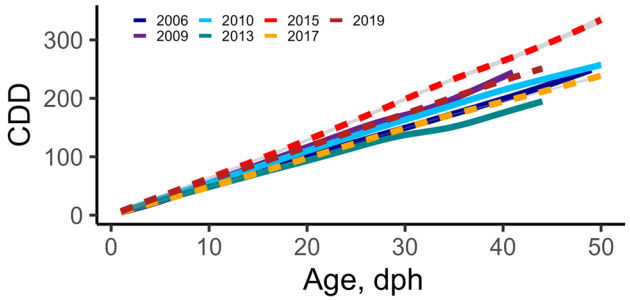

Figure 9. Cumulative Degree Days (CDD) by age, in days post hatch (dph). Years before (2006, 2009, 2010, 2013) the marine heatwaves are represented by solid blue lines and years during & between (2015, 2017, 2019) MHWs are represented by dashed, red lines.

initiation (Fig. 10a $r = 0.800$, $n = 7$, $P = 0.095$). Larvae grew faster when bloom initiation occurred later in the year as indicated by a positive correlation between mean absolute growth rates (mm/day) and bloom initiation (Fig. 10b, $r = 0.906$, $n = 7$, $P = 0.025$). Growth rates were also faster when hatch dates occurred later in the year (Fig. 10c, $r = 0.960$, $P = 0.004$) and tended to be higher when mean SST temperature was lower, as indicated by a weak negative correlation (Fig. 10d, $r = -0.740$, $P = 0.115$).

Discussion

Understanding the effects of MHWs throughout the life history of fishes is integral to realistic future management projections[33]. The dramatic decline in the GOA Pacific cod population after two extreme MHWs, which resulted in a federal disaster declaration for the fishery, provided an opportunity to better understand individual responses to acute ocean warming. Reduced spawning activity and/or hatching success coupled with severe metabolic stress of adult fish are often cited as key factors contributing to that population decline[8]. However, we also observed notable shifts in hatching phenology (~ 3 weeks earlier) and interactive effects of hatch date and age on growth

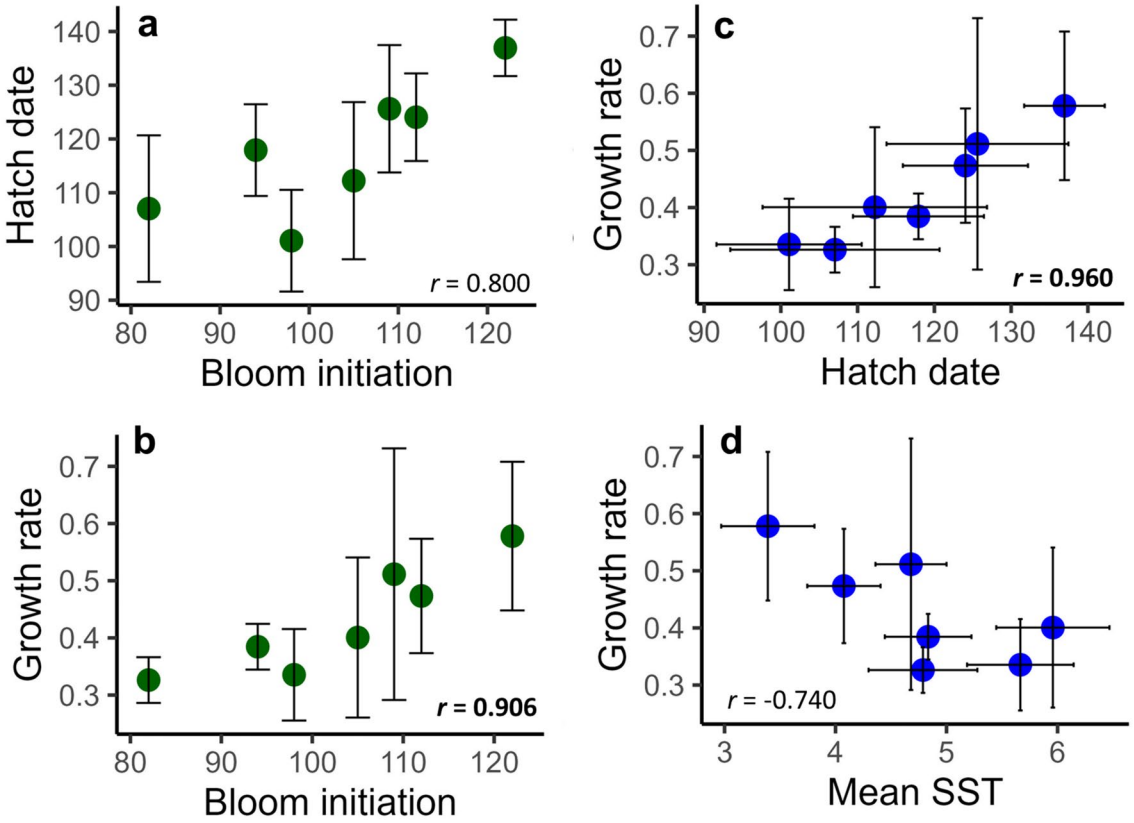

Figure 10. Scatterplots of mean (SD) annual values for (**a**) timing of bloom initiation in the Gulf of Alaska and larval hatch dates; (**b**) timing of bloom initiation and annual absolute larval growth rates (mm/day); (**c**) hatch dates and larval growth rates (mm/day); and (**d**) sea surface temperature (SST, °C) January through April and larval growth rates (mm/day). Correlations with $P < 0.005$ are in bold.

and size of larvae during warmer ocean conditions. These complex interactions with temperature could also influence the size and condition of older age classes, affecting the demography and productivity of the population[34].

We documented a nearly three-week (19 d) shift in hatch dates of GOA larval Pacific cod between 2006 and 2019, which was associated with the onset of the 2014–2016 MHW. Our comparisons are limited to every other year given the biennial frequency of the larval survey. However, the mean hatch date shifted 11 days earlier from 2013 to 2015, and hatch dates were even earlier in 2017 and 2019. The greatest difference in mean hatch dates (36 days) occurred between the coldest (2009) and warmest (2019) years. Examination of the phenology of 43 fish species in the California Current between 1951 and 2008 reported phenological shifts in 26 species[40]. For species with earlier hatch dates, the rate of change was between −2.8 to −12.4 days per decade (mean = −6.4), which translated to a temperature sensitivity that ranged from 10.8 to 47.7 days per ℃. An examination[35] of the reproductive phenology of walleye pollock (*Gadus chalcogrammus*), which can spawn multiple times in a season, over 32 years found that a 1 ℃ increase in March SST corresponded to a 5-day shift to earlier spawning. For Pacific cod from 2006 to 2019, we observed a shift of 14.7 days in hatch phenology per 1 ℃ increase in January to April deep temperatures, which aligns with prior studies. In addition to temperature, population demographics were important with an older and more age-diverse spawning stock related to earlier spawning for longer duration in walleye pollock[35]. However, there is no evidence that the age composition of Pacific cod spawners has shifted during & between the MHWs and affected reproductive phenology[11].

Shifts in hatching phenology for nearshore collections of juvenile Pacific cod collected in July in the GOA from 2006 to 2019 were 14 to 28 d earlier since 2015[20], which are notably similar to our observations for offshore larvae collected in May. However, although the phenological shifts in hatch time were similar for both life stages, larvae in our study hatched, on average, a month later than the juveniles. This consistent shift in phenology within, but offset between, life stages could be explained by several factors. The larvae could (1) be from a different source population than the juveniles; (2) represent later spawners within the population; (3) indicate that there was selection on hatch date between May and July; (4) or a combination of these factors. However, the idea that selective mortality on hatch date associated with MHWs across multiple years was so consistent for larvae and juveniles that hatched approximately one month apart seems unlikely. Additionally, in both studies, direct effects of temperature during incubation could only account for a portion of these shifts in phenology. Overall, the consistent temporal shift in phenology observed for both larvae and juveniles indicates that, at least in the northern GOA, the effect of the MHWs on hatching phenology was similar and likely related to changes in parental spawning timing, such as increased gonadal developmental rates and behavioral differences, embryonic developmental rates, and potentially selection associated with hatch date.

The similar shifts in hatch date observed for Pacific cod larvae and juveniles, even if offset by a month, have important and encouraging implications for survey design. Our larvae were collected by National Oceanic and Atmospheric Administration's (NOAA) Alaska Fisheries Science Center's (AFSC) as part of a long-term survey focused on walleye pollock, which spawns later than Pacific cod[35]. While the precise timing and duration of larval production may be difficult to discern for non-target species, the similar temporal shifts evident in larval and juvenile collections indicate that long-term survey data can provide insights on the effects of acute—and likely longer-term—warming on reproductive phenology. Even surveys that do not capture peak larval production may be able to provide estimates of phenological shifts in reproduction, at least for single-batch spawners such as Pacific cod.

The slower growth and smaller size-at-age we observed during warmer periods could be related to reductions in the quantity or quality of prey or a mismatch in timing of production[36,37]. Reductions in early growth with warming are expected if prey resources are inadequate to meet metabolic demands[38]. Changes in the timing and magnitude of the phytoplankton bloom during MHWs could influence the timing, quantity, or quality of secondary production, which includes the prey of larval Pacific cod[32,39,40]. The positive correlations observed between growth rates and hatch dates and the date of bloom initiation suggest match-mismatch dynamics may be important, but more data are needed. As noted earlier, juvenile Pacific cod in the GOA had similar patterns of slower larval growth very early in life since 2015[20]. However, those juveniles hatched about one month earlier than our larvae. Therefore, the factors influencing slower larval growth during MHWs appear to have persisted for at least a month.

Marine fish larvae increase visual foraging capacity as they develop, and daylength can further affect their foraging opportunities and subsequent growth[41]. The earliest observed mean hatch date (11 April) experienced approximately two hours less daylength than the latest mean hatch date (17 May), which likely led to reduced opportunities to forage. Laboratory-reared pre-flexion Pacific cod larvae that were similar in age (0 to 36 dph) to the those in this study (mean = 22 dph) were maintained at 2 to 8 ℃ and fed enriched rotifers and dry food at least twice daily[42]. Their daily absolute growth rates were less than 0.20 mm/day at all temperatures whereas GOA larvae in this study, which primarily experienced temperatures < 8 ℃, had mean overall growth rates (0.32 to 0.58) that were 30 to nearly 300% faster than the well-fed laboratory larvae. Therefore, while we observed slower growth associated with the onset of MHWs in 2015, larval growth rates were not unusually low in any year, indicating that surviving larvae were able to find adequate food, as suggested by others[43].

If earlier hatchers experience shorter daylength, slower growth, and potentially reduced foraging opportunities, why do they persist? During cooler conditions, late hatchers had a growth advantage early in life (Fig. 6). However, as waters warmed, the overall growth variation during early life declined and growth rates converged at ~ 0.04 mm/mm/day. The convergence of early growth was not due to slower growth for later hatchers but rather due to faster growth rates for earlier hatchers during warmer conditions. Furthermore, growth rates of early hatchers during warmer temperatures did not exceed growth rates of later hatchers during cooler conditions. Therefore, earlier hatching during warming may lead to increases in growth (relative to later hatchers) that could contribute to their overall survival. Once conditions change (warm) and allow for increased growth

of earlier hatchers, survivors would have subsequent size advantages due to their older age that could enhance later survival.

When examined through the lens of CDD, it is notable that the CDD-at-age was relatively similar across years with the exception of 2015, which was also the first year the MHWs directly affected larvae as the MHW began late in 2014. Hatch dates in 2015 coincided with a sharp increase in surface temperatures (Fig. 2), which exceeded all other years and likely contributed to the greater overall thermal exposure that year. Although bottom temperatures were similar during the MHW years 2015 and 2019, surface waters warmed faster and attained higher temperatures in 2015. Larval CPUE was also lowest during 2015, which was the first year that spawning occurred during the MHW, indicating poor hatching success and/or early larval survival.

Various mechanisms are proposed for the TSR, which refers to global observations of reduced size- and age-at-maturity and larger body size early in life. These include physiological (increased metabolic rates and associated oxygen demand), environmental (decreased oxygen availability and subsequent selection for smaller body size), and ecological (shifts in prey composition or mortality rates) processes[44–47]. However, there are relatively few field observations that quantify how both shifts in phenology and individual growth influence body size during warming. Our results highlight that shifts in hatching phenology can wholly account for larger larval size observed in long-term surveys. Additionally, stage-specific larval growth rates did not increase with temperature and were similar regardless of marine heatwave status. On the other hand, a similar study on Atlantic cod (*Gadus morhua*) found that growth rates, rather than hatch dates, could explain differences in body size of juveniles collected with the North Sea[48]. These variable responses in phenology and growth have important implications for the use of temperature-dependent growth responses to predict individual, population, and community responses to climate change[49,50].

Although moderately faster juvenile growth rates during warming have been reported in laboratory and field studies[41,51], the TSR is less clear on expectations for larval stages and many field observations of body size are reported without daily age estimates. The smaller size-at-age during warmer periods that we observed in larval Pacific cod could be related to more rapid embryonic development leading to smaller size-at-hatch, which aligns with observations of more rapid development at warmer temperatures[52–54]. If this was the primary cause, it would be reasonable to expect growth rates to increase later in life, such as after metamorphoses, which occurs at ~ 25 to 30 mm TL in Pacific cod[55] (NOAA, 2024). However, during & between the MHWs, GOA juvenile Pacific cod also grew more slowly until 50 to 60 dph when relative growth rates increased for a few weeks but converged again by ~ 80 dph[20]. Therefore, while faster development likely contributed to our results, other factors contributed to the slower early growth in Pacific cod during MHWs.

Shifts in hatch phenology alone can have notable effects on size that carry over to older ages. These age-related size differences can influence body size when fish enter their first winter and could contribute to observations of increased size-at-age early in life. For example, most comparisons of size-at-age, particularly age-1 fish, assume individuals are the same age. However, individuals that hatch nearly three weeks earlier in a warmer year would be older, and notably larger, during their first winter than fish from a cooler year. For age estimation, the formation of the first annulus in an otolith is assumed to occur during winter, often January 1[56]. However, if a fish is 30 or 40 days older by January 1 and growing conservatively at an average of 0.40 mm/day, that individual could be 12 to 16 mm longer due to earlier hatch date alone. Hence, greater body size associated with older daily age alone could carry over into older age classes, potentially contributing to observations of larger size-at-age before maturity during warmer conditions. While faster growth is an often-cited mechanism regulating observations underpinning the TSR, the effect of shifting phenology and fish that are effectively older at "age-1" warrant further consideration.

An important consideration is how reflective MHWs are of longer-term warming conditions. While acute warming events can be informative, there are key differences associated with the more sudden onset of warming events that result in less time for acclimation and may result in stronger selection for certain traits under extreme conditions. During warmer periods, regardless of the cause, there is the potential for elevated metabolism and predators and prey may require higher consumption rates to maintain growth. However, longer-term warming could be associated with shifts in community composition of both predators and prey and provide more time for movement and adaptation. Overall, acute events such as MHWs provide an important opportunity to learn about how individuals and populations respond to warming and test key hypotheses, such as the TSR, and become better informed about the consequences of longer-term ocean warming, although there are some limitations to the comparison.

Our study highlights the importance of information on individual age and growth from long-term surveys to understand organismal and population responses to warming. The fact that older age alone can account for increases in larval body size observed during & between the MHWs emphasizes the importance of phenological change and age determination when evaluating the effects of warming on early life stages. The complex interactions among hatch date, age, and temperature underscore how growth can be affected in unexpected ways. Although size- and temperature-dependent growth models based on laboratory studies can be informative[57], we observed similar growth across temperatures before and during & between MHWs, which indicates that comprehensive efforts to understand the effects of warming cannot rely solely on such approaches to generate accurate predictions.

Methods

Larval collection

Archived samples of larval Pacific cod, collected by the National Oceanic and Atmospheric Administration's (NOAA) Alaska Fisheries Science Center's (AFSC) Ecosystems and Fisheries-Oceanography Coordinated Investigations Program (EcoFOCI), were used for this study. Samples were collected with a 60 cm paired bongo frame

equipped with either 333- or 505-µm mesh nets and flow meters. The net was towed obliquely at evenly spaced, predetermined sites to 100 m depth or 10 m off bottom in shallower water. One of the paired bongo nets was preserved in ethanol while the other net was preserved in 5% buffered formalin and larval Pacific cod were subsequently sorted, counted, and measured for total length (TL) to the nearest millimeter at the Plankton Sorting and Identification Center in Szczecin, Poland. Lengths were corrected for shrinkage associated with formalin preservation ($TL_{corrected} = 1.044 \cdot TL_{preserved} + 0.530$, $n = 57$, $R^2 = 0.947$). The spatial area sampled included the Shelikof Strait and associated sea valley to east of the Shumagin Islands (Fig. 1). Larval counts were standardized to number per 10 m^2 sea surface area as a measure of catch per unit effort (CPUE). Since 2013, the survey in the GOA has occurred in odd years only.

The larvae used in this study were collected through a long-term governmental plankton monitoring program by federal scientists at the NOAA's AFSC under a National Marine Fisheries Service Scientific Research Permit. All research was carried out in accordance with applicable guidelines and regulations at the time that the study was conducted. Oregon State University's Institutional Animal Care and Use Committee (IACUC) approved of this study through an exemption because samples were provided after collection. Larvae were deceased by the time nets were retrieved and rinsed and were immediately preserved in ethanol or 5% buffered formalin. All methods are reported in accordance with ARRIVE guidelines (https://arriveguidelines.org).

Otolith preparation and interpretation

Larval Pacific cod from ethanol-preserved samples were available from May surveys that occurred in 2006, 2009, 2010, 2013, 2015, 2017, and 2019. The duration of the surveys ranged from 9 to 19 days with a mean of 12.9 days ± 4.2 SD. All available otoliths from years with fewer than 20 larvae were included along with a random sample of at least 20 individuals from years with more than 20 larvae (Table 1). Larvae were imaged, measured for TL to the nearest 0.1 mm, and otoliths were extracted. Total lengths were corrected for shrinkage associated with ethanol preservation ($TL_{corrected} = 1.030 \cdot TL_{preserved} + 0.612$, $n = 52$, $R^2 = 0.947$). We prepared thin sections by mounting sagittae on glass slides with thermoplastic resin, polishing the distal side, flipping the otolith, and polishing the proximate side to expose the core region. We used 3 M™ Wetordry™ paper (1000–2000 grit), Buehler® lapping film (3-to-30-micron), and alumina slurry (0.3 micron). Polished otolith sections were imaged (Levenhuk® T300 camera) with a compound microscope at 100X and 400X magnification. Daily otolith increment formation has been validated for Pacific cod[58]. Therefore, we measured the radius and counted all daily increments to estimate individual age. Every otolith was read by one to three readers one to two times using ImagePro Premier®. If independent counts varied by > 10%, otoliths were revisited, and discrepancies were resolved. The final read used to provide age and increment widths for subsequent analyses was randomly selected from multiple reads per individual.

There were strong, positive, linear relationships between larval size and otolith radius for each year of the study (Supplementary Fig. S1). Therefore, we used the biological-intercept back-calculation model[59] with published values for Pacific cod biological intercepts[58] to estimate fish size at each day of life based on otolith radii measurements. Hatch date estimates were generated by subtracting age from the day of capture. We then estimated a daily growth rate for each individual based on daily change in size. We calculated a daily growth rate (mm/day) and a relative growth rate (mm/mm/day) to reduce the effect of size on growth rate.

Temperature

To characterize thermal history of each larvae, we estimated daily mean temperature by interpolating monthly data from the oceanographic station GAK1 (Fig. 2), which is the longest and most complete seasonal temperature record for the GOA and reflects regional temperature patterns[17] (research.cfos.uaf.edu/gak1/data/TimeSeries/). We selected depths to align with larval growth based on the life history of Pacific cod, which spawn in relatively deep waters (75–250 m)[60–62]; and hatch near the sea floor[16] before moving towards the surface relatively quickly[42,43]. Therefore, we used mean temperatures at depths from 100 to 250 m for the first 5 dph and temperatures from 0 to 30 m from 6 dph to capture. This approach allowed us to assign a daily mean temperature to each day of life for every larva. We grouped larvae according to MHW status, which was evaluated using the R package '*heatwaveR*'[63].

Relationships with annual phytoplankton bloom

We used metrics of the annual phytoplankton bloom in the GOA as an indicator of relative productivity. The metrics were based on spatial and temporal characteristics of surface chlorophyll *a* (Chl *a*) measured with satellite remote sensing data spanning the MODIS era[36]. The area for the bloom metric represents the entire GOA shelf region < 300 m between 150°W and 170°W. Satellite chlorophyll estimated with MODIS-Aqua (years 2003–2019: R2018.0) were obtained from the NASA OceanColorWeb (https://oceancolor.gsfc.nasa.gov). Spatial resolution of the ocean color products was approximately 9 km with an 8 day average for the temporal resolution. The start and end dates of the surface expression of the bloom were defined as the day Chl *a* biomass reached one-third and one-half of the annual maximum, respectively. The duration was the number of days between the start and end dates. We compared these annual estimates of the bloom initiation date and duration with estimates of annual mean larval hatch date and absolute growth rate (total length at capture (mm) / age = mm/day) with using Pearson correlation analysis with Bonferroni correction for multiple comparisons. We also calculated an overall mean temperature for surface waters (0 to 30 m) based on GAK1 temperatures during January to April ($T_{J\text{-}A,SST}$) for comparison with the larval metrics.

Age and hatch phenology

We developed an age-length model based on otolith-aged fish with year of capture as a fixed effect ($R^2 = 0.88$, $n = 201$, Supplementary Table S6), which was used to estimate age of the remaining larvae based on their formalin-corrected length ($n = 2061$). To determine if hatch dates changed during and between MHWs, we used a LMM to examine variation in hatch date in relation to MHW status ("before" and "during & between"). We compared models with various random effects, including year, station, station nested in year, and all combinations using Akaike Information Criteria (AIC) and maximum likelihood (ML). The most parsimonious model included MHW status as a fixed effect and year and station as random effects (AIC = 16,077 versus > 16,170 for all other models). The final model was estimated using restricted maximum likelihood (REML) and an nlminb optimizer.

Based on the GAK1 temperature record, we generated a mean temperature at deeper depths (100 to 250 m) from January to April ($T_{\text{J-A, 100-250 m}}$), which covers the majority of the spawning and incubation period. We also estimated mean annual incubation temperatures to determine what proportion of the observed differences in hatch dates across years could be attributed to direct effects of temperature on embryonic development. Based on laboratory studies[58,64], Pacific cod hatch after a mean of 110 ℃ degree days. Therefore, for each individual ($n = 2262$), we estimated the number of days prior to hatching required to attain 110 ℃ degree days using our estimated hatch dates and GAK1 temperature data (100 to 250 m depth). We then examined the pairwise mean difference in the number of days to attain 110 ℃ degree days with observed hatch dates across years to estimate the proportion of the shifts in hatch date that could be attributed to direct effects of temperature on development. Finally, to further examine the relationship between hatch dates and temperature across years, we conducted a simple linear regression between mean annual hatch date and $JT_{\text{J-A, 100-250 m}}$ and between mean annual hatch date and incubation temperatures to determine which metric best described interannual variation in hatch dates ($n = 7$).

Size-at-age

We expected larvae to be larger-at-age during & between MHWs due to faster growth at warmer temperatures. To test this hypothesis, we examined the effect of MHW status on size-at-age using a LMM to predict length at capture. The use of standardized parameters results in the variable having a mean of 0 and a standard deviation of 1, which puts them in similar ranges and is helpful when models contain polynomial terms or interaction terms. It can also help compare effects in LMM because estimated coefficients are on the same scale. We compared models with and without year and station as random effects using maximum likelihood (ML) and fit the most parsimonious model with REML. Ninety-five percent Confidence Intervals (CIs) and p-values were computed using a Wald t-distribution approximation. We present marginal mean size-at-age, which represent the predicted size averaged across ages before and during & between the MHWs, along with observed data.

Growth

To examine factors influencing daily growth, we used a LMM to predict daily relative growth (mm/mm/day). We evaluated models with age, daily temperature, hatch date, and all interactions as fixed effects with day of life nested in fish ID as a random effect. Given that nearly 30% of the stations had only one individual, we did not consider a random effect for station in this model[65]. We also compared models with and without a first order autocorrelation function to account for growth correlation within individuals. Standardized parameters were obtained by fitting the model with standardized covariates to aid in model interpretation. We considered models that included MHW status as a factor, but they had moderate to high collinearity (Variable Inflation Factors, VIF > 5) and, therefore, were excluded. All models were compared using AIC with maximum likelihood functions, and the final model was then fitted using REML and an nlminb optimizer. We estimated marginal means, which represent the average predicted relative daily growth for specific ages, hatch dates, and temperatures.

In order to better visualize differences in relative growth before and during & between MHWs, we present the data in two additional ways. First, we binned all data into three groups for temperature (< 5.0 ℃, between 5.0 and 5.7 ℃ and > 5.7 ℃) and for hatch date ("Early" = 6 March to 15 April, "Middle" = 16 April to 27 April, and "Late" = 28 April to 21 May), with each bin including ~ 33% of the observations. We then plotted observed and predicted relative growth from the LMM described above by age across the three temperature and hatch date groups before and during & between MHWs. Second, to visualize growth at similar temperatures before and during & between the MHWs, we plotted observed relative growth by temperature for larvae at 6 to 20 dph and at 31 to 45 dph and grouped by the same three hatch date groups. The mean size for the 6 to 20 day old larvae was 9.9 (2.2 SD) and for the 31 to 45 day old larvae was 12.8 (2.0). For this plot, we fit simple linear models to observed data rather than predictions for visualization purposes. We did not use output from the LMM in this plot because we wanted to examine growth responses across temperature directly, rather than based on predictions that accounted for temperature.

Lifetime thermal history using Cumulative Degree Day (CDD)

To compare larval size and growth in relation to lifetime thermal exposure, we calculated Cumulative Degree Days (CDD) for each day of life for every larva. The daily mean temperature for each day of life of every individual was summed, generating a daily estimate of CDD for each larva. As in the growth analysis, we used the mean temperatures at depths from 100 to 250 m for the first 5 dph and temperatures from 0 to 30 m from 6 dph to capture. We plotted CDD by age in order to visualize variation in lifetime thermal exposure across years.

Statistical analyses

All analyses were conducted in R (version 4.2.2), and we visualized our results with R package '*ggplot*' (version 3.4.4)[66]. All models were developed using the R package '*nlme*' (version 3.1–160)[67] except for the growth models,

which were developed using the R package '*lme4*' (version 1.1.31)[68]. We examined residuals and quantile–quantile (QQ) plots of all models and evaluated multicollinearity with VIF. Marginal model means were generated with the R packages '*effects*'[69] and '*ggeffects*' [70].

Data availability

Data and code are publicly available via GitHub (www.GitHub.com) at https://github.com/millerjessicaadele/Data-Code-for-Age-not_Growth.

Received: 14 June 2024; Accepted: 9 August 2024
Published online: 20 August 2024

References

1. Di Lorenzo, E. & Mantua, N. Multi-year persistence of the 2014/15 North Pacific marine heatwave. *Nat. Clim. Change* **6**, 1042–1047 (2016).
2. Oliver, E. C. J. *et al.* Longer and more frequent marine heatwaves over the past century. *Nat. Commun.* **9**, 1324. https://doi.org/10.1038/s41467-018-03732-9 (2018).
3. Xu, T. *et al.* An increase in marine heatwaves without significant changes in surface ocean temperature variability. *Nat. Commun.* **13**, 7396. https://doi.org/10.1038/s41467-022-34934-x (2022).
4. Smith, K. E. *et al.* Biological impacts of marine heatwaves. *Annu. Rev. Mar. Sci.* **15**, 119–145 (2023).
5. Smith, K. E. *et al.* Socioeconomic impacts of marine heatwaves: global issues and opportunities. *Science* **374**, 6566. https://doi.org/10.1126/science.abj3593 (2021).
6. Suryan, R. M. *et al.* Ecosystem response persists after a prolonged marine heatwave. *Sci. Rep.* **11**, 6235. https://doi.org/10.1038/s41598-021-83818-5 (2021).
7. Litzow, M. A. *et al.* Evaluating ecosystem change as Gulf of Alaska temperature exceeds the limits of preindustrial variability. *Prog. Ocean.* https://doi.org/10.1016/j.pocean.2020.102393 (2020).
8. Barbeaux, S. J., Holsman, K. & Zador, S. Marine heatwave stress test of ecosystem-based fisheries management the Gulf of Alaska Pacific cod fishery. *Front. Mar. Sci.* https://doi.org/10.3389/fmars.2020.00703 (2020).
9. Peterson Williams, M. J., Robbins Gisclair, B., Cerny-Chipman, E., LeVine, M. & Peterson, T. The heat is on: Gulf of Alaska Pacific cod and climate-ready fisheries. *ICES J. Mar. Sci.* **79**, 573–583 (2022).
10. Free, C. M. *et al.* Impact of the 2014–2016 marine heatwave on US and Canada West coast fisheries: Surprises and lessons from key case studies. *Fish Fish.* **24**, 652–674 (2023).
11. Hulson, P. J. F., Barbeaux, S. J., Ferriss, S., McDermott, S. F. & Spies, I. B. Assessment of the Pacific cod stock in the Gulf of Alaska. https://apps-afsc.fisheries.noaa.gov/Plan_Team/2022/GOApcod.pdf (2022).
12. Hughes, A. R. *et al.* Predicting the sensitivity of marine populations to rising temperatures. *Front. Ecol. Environ.* **17**, 17–24 (2019).
13. Levangie, P. E. L., Blanchfield, P. J. & Hutchings, J. A. The influence of ocean warming on the natural mortality of marine fishes. *Env. Biol. Fish.* **105**, 1447–1461 (2022).
14. Maschner, H. D. G., Betts, M. W., Reedy-Machner, K. L. & Trites, A. W. A 4500-year time series of Pacific cod (*Gadus macrocephalus*) size and abundance: Archaeology, oceanic regime shifts, and sustainable fisheries. *Fish. Bull.* **106**, 386–394 (2008).
15. West, C. F., Etnier, M. A., Barbeaux, S., Partlow, M. A. & Orlov, A. M. Size distribution of Pacific cod (*Gadus macrocephalus*) in the North Pacific Ocean over 6 millennia. *Quat. Res.* https://doi.org/10.1017/qua.2020.70 (2020).
16. Bian, X. *et al.* Temperature-mediated survival, development and hatching variation of Pacific cod *Gadus macrocephalus* eggs. *J. Fish Biol.* **84**, 85–105 (2014).
17. Laurel, B. J. & Rogers, L. A. Loss of spawning habitat and prerecruits of Pacific cod during a Gulf of Alaska heatwave. *Can. J. Fish. Aquat. Sci.* **77**, 644–650 (2020).
18. Doyle, M. & Mier, K. A new conceptual framework for evaluating the early ontogeny phase of recruitment processes among marine fish species. *Can. J. Fish. Aquat. Sci.* **69**, 2112–2129 (2012).
19. Abookire, A. A., Litzow, M. A., Malick, M. J. & Laurel, B. J. Post-settlement abundance, condition, and survival in a climate-stressed population of pacific cod. *Can. J. Fish. Aquat. Sci.* **79**, 958–968 (2022).
20. Almeida, L. Z., Laurel, B. J., Thalmann, H. L. & Miller, J. A. Warmer, earlier, faster: Cumulative effects of Gulf of Alaska heatwaves on the early life history of Pacific cod. *Elem. Sci. Anth.* **12**, 1. https://doi.org/10.1525/elementa.2023.00050 (2024).
21. Doyle, M. J. *et al.* Early life history phenology among Gulf of Alaska fish species: Strategies, synchronies, and sensitivities. *Deep-Sea Res. II* **165**, 41–73 (2019).
22. Laurel, B. J. *et al.* Pacific cod in the Anthropocene: An early life history perspective under changing thermal habitats. *Fish Fish.* **24**, 959–978 (2023).
23. Hastings, R. A. *et al.* Climate change drives poleward increases and equatorward declines in marine species. *Curr. Biol.* **30**(8), 1572–1577 (2020).
24. Stabeno, P. J., Reed, R. K. & Napp, J. M. Transport through Unimak Pass. *Alaska. Deep-Sea Res. II* **49**, 5919–5930 (2002).
25. Atkinson, D. Temperature and organism size—a biological law for ectotherms? In *Advances in Ecological Research* (eds Begon, M. & Fitter, A. H.) (Academic Press, 1994).
26. Atkinson, D., Morley, S. A. & Hughes, R. N. From cells to colonies: at what levels of body organization does the 'temperature-size rule' apply? *Evol. Develop.* **8**, 202–214 (2006).
27. Thalmann, H. L. *et al.* Marine heatwaves alter the nursery function of coastal habitats for juvenile Gulf of Alaska Pacific cod. *Sci. Rep.* **14**, 14018. https://doi.org/10.1038/s41598-024-63897-w (2024).
28. Hobday, A. J. *et al.* A hierarchical approach to defining marine heatwaves. *Prog. Ocean.* **141**, 227–238 (2016).
29. Hobday, A. J. *et al.* Categorizing and naming marine heatwaves. *Ocean.* **31**, 2. https://doi.org/10.5670/oceanog.2018.205 (2018).
30. Bonhomme, R. Bases and limits to using 'degree.day' units. *Eur. J. Agron.* **13**, 1–10 (2000).
31. Venturelli, P. A., Lester, N. P., Marshall, T. R. & Shuter, B. J. Consistent patterns of maturity and density-dependent growth among populations of walleye (*Sander vitreus*): application of the growing degree-day metric. *Can. J. Fish. Aquat. Sci.* **67**, 1057–1067 (2010).
32. Takatsu, T., Nakatani, T., Mutoh, T. & Takahashi, T. Feeding habits of Pacific Cod larvae and juveniles in Mutsu Bay. *Jpn. Fish. Sci.* **61**, 415–422 (1995).
33. van Denderen, D., Gislason, H., van den Heuvel, J. & Andersen, K. H. Global analysis of fish growth rates shows weaker responses to temperature than metabolic predictions. *Glob. Ecol. Biogeog.* **29**, 2203–2213 (2020).
34. Moore, M. P. & Martin, R. A. On the evolution of carry-over effects. *J. Anim. Ecol.* **88**, 1832–1844 (2019).
35. Rogers, L. A. & Dougherty, A. B. Effects of climate and demography on reproductive phenology of a harvested marine fish population. *Glob. Change Biol.* **25**, 708–720 (2019).
36. Laurel, B. J. *et al.* Regional warming exacerbates match/mismatch vulnerability for cod larvae in Alaska. *Prog. Ocean.* https://doi.org/10.1016/j.pocean.2021.102555 (2021).

37. Cushing, D. H. Plankton production and year-class strength in fish populations: An update of the match/mismatch hypothesis. *Adv. Mar. Biol.* **26**, 249–293 (1990).
38. Shelley, C. E. & Johnson, D. W. Larval fish in a warming ocean: A bioenergetic study of temperature-dependent growth and assimilation efficiency. *Mar. Ecol. Prog. Ser.* **691**, 97–114 (2022).
39. Neuheimer, A. B., MacKenzie, B. R. & Payne, M. R. Temperature-dependent adaptation allows fish to meet their food across their species' range. *Sci. Adv.* **4**, 7. https://doi.org/10.1126/sciadv.aar4349 (2018).
40. Asch, R. G., Stock, C. A. & Sarmiento, J. L. Climate change impacts on mismatches between phytoplankton blooms and fish spawning phenology. *Glob. Change Biol.* **25**, 2544–2559 (2019).
41. Shoji, J. *et al.* Possible effects of global warming on fish recruitment: shifts in spawning season and latitudinal distribution can alter growth of fish early life stages through changes in daylength. *ICES J. Mar. Sci.* **68**, 1165–1169 (2011).
42. Hurst, T. P., Laurel, B. J. & Ciannelli, L. Ontogenetic patterns and temperature-dependent growth rates in early life stages of Pacific cod (*Gadus macrocephalus*). *Fish. Bull.* **108**, 382–392 (2010).
43. Doyle, M. J. & Mier, K. L. Early life history pelagic exposure profiles of selected commercially important fish species in the Gulf of Alaska. *Deep-Sea Res.* **II**(132), 162–193 (2016).
44. Angilletta, M. J. Jr., Steury, T. D. & Sears, M. W. Temperature, growth rate, and body size in ectotherms: Fitting pieces of a life-history puzzle. *J. Integral. Compare. Biol.* **44**, 498–509 (2004).
45. Ghosh, S. M., Testa, N. D. & Shingleton, A. W. Temperature-size rule is mediated by thermal plasticity of critical size in *Drosophila melanogaster*. *Proc. Royal Soc. B: Biol. Sci.* https://doi.org/10.1098/rspb.2013.0174 (2013).
46. Baudron, A. R., Needle, C. L., Rijnsdorp, A. D. & Tara Marshall, C. Warming temperatures and smaller body sizes: Synchronous changes in growth of North Sea fishes. *Glob. Change Bio.* **20**, 1023–1031 (2014).
47. Audzijonyte, A., Jakubavičiūtė, E., Lindmark, M. & Richards, S. A. Mechanistic temperature-size rule explanation should reconcile physiological and mortality responses to temperature. *Biol. Bull.* **243**, 2. https://doi.org/10.1086/722027 (2022).
48. Jørgensen, K. E. M., Neuheimer, A. B., Jorde, P. E., Knutsen, H. & Grønkjær, P. Settlement processes induce differences in daily growth rates between two co-existing ecotypes of juvenile cod *Gadus morhua*. *Mar. Ecol. Prog. Ser.* **650**, 175–189 (2020).
49. Reum, J. C. P. *et al.* Temperature-dependence assumptions drive projected responses of diverse size-based food webs to warming. *Earth's Future* https://doi.org/10.1029/2023EF003852 (2024).
50. Gomes, D. G. E. *et al.* Marine heatwaves disrupt ecosystem structure and function via altered food webs and energy flux. *Nat. Comm.* **15**, 1988. https://doi.org/10.1038/s41467-024-46263-2 (2024).
51. Ong, J. J. L. *et al.* Contrasting environmental drivers of adult and juvenile growth in a marine fish: Implications for the effects of climate change. *Sci. Rep.* **5**, 10859. https://doi.org/10.1038/srep10859 (2015).
52. Pepin, P. Effect of temperature and size on development, mortality, and survival rates of the pelagic early life history stages of marine fish. *Can. J. Fish. Aquat. Sci.* **48**, 503–518 (1991).
53. McLeod, I. M. *et al.* Latitudinal variation in larval development of coral reef fishes: implications of a warming ocean. *Mar. Ecol. Prog. Ser.* **521**, 129–141 (2015).
54. Fennie, H. W., Grorud-Colvert, K. & Sponaugle, S. Larval rockfish growth and survival in response to anomalous ocean conditions. *Sci. Rep.* **13**, 4089. https://doi.org/10.1038/s41598-023-30726-5 (2023).
55. NOAA. *Ichthyoplankton Information System*. Online at https://apps-afsc.fisheries.noaa.gov/ichthyo/index.php (2024).
56. CARE (Committee of Age Reading Experts). *Manual of Generalized Age Determination: Procedures for Groundfish*. 52; Online at https://care.psmfc.org/docs/CareManual2006.pdf (2006).
57. Folkvord, A. Comparison of size-at-age of larval Atlantic cod (*Gadus morhua*) from different populations based on size- and temperature-dependent growth models. *Can. J. Fish. Aquat. Sci.* **62**, 1037–1052 (2005).
58. Narimatsu, Y., Hattori, Y., Ueda, H., Matsuzaka, M. & Shigaki, M. Somatic growth and otolith microstructure of larval and juvenile Pacific cod *Gadus macrocephalus*. *Fish. Sci.* **73**, 1257–1264 (2007).
59. Campana, S. E. How reliable are growth back-calculations based on otoliths? *Can. J. Fish. Aquat. Sci.* **47**, 2219–2227 (1990).
60. Ketchen, K. S. Observations on the ecology of the Pacific cod (*Gadus macrocephalus)* in Canadian waters. *J. Fish. Res. Board Can.* **18**(4), 513–558 (1961).
61. Stark, J. W. Geographic and seasonal variations in maturation and growth of female Pacific cod (*Gadus macrocephalus*) in the Gulf of Alaska and Bering Sea. *Fish. Bull.* **105**, 396–407 (2007).
62. Neidetcher, S. K., Hurst, T. P., Ciannelli, L. & Logerwell, E. A. Spawning phenology and geography of Aleutian Islands and eastern Bering Sea Pacific cod (*Gadus macrocephalus*). *Deep-Sea Res.* **II**(109), 204–214 (2014).
63. Schlegel, R. W. & Smit, A. J. HeatwaveR: A central algorithm for the detection of heatwaves and cold-spells. *J. Open Source Soft.* **3**, 821. https://doi.org/10.2110/joss.00821 (2018).
64. Laurel, B. J., Hurst, T. P., Copeman, L. A. & Davis, M. W. The role of temperature on the growth and survival of early and late hatching Pacific cod larvae (*Gadus macrocephalus*). *J. Plank. Res.* **30**, 1051–1060 (2008).
65. Bolker, B. M. *et al.* Generalized linear mixed models: A practical guide for ecology and evolution. *Trends Ecol. Evol.* **24**, 127–135 (2009).
66. Wickham, H. *Ggplot2: Elegant Graphics for Data Analysis* (Springer-Verlag, 2016).
67. Pinheiro, J. & Bates, D. nlme: linear and nonlinear mixed effects models. R package version 3.1–164. Online at https://svn.r-project.org/R-packages/trunk/nlme/ (2023).
68. Bates, D., Mächler, M., Bolker, B. M. & Walker, S. Fitting linear mixed-effects models using lme4. *J. Stat. Soft.* **67**, 1–48. https://doi.org/10.18637/jss.v067.i01 (2015).
69. Fox, J. & Weisberg, S. *An R Companion to Applied Regression* (Sage Publications, 2019).
70. Lüdecke, D. ggeffects: Tidy data frames of marginal effects from regression models. *J. Open Source Soft.* https://doi.org/10.21105/joss.00772 (2018).

Acknowledgements

We thank T. Murphy and T. Brooks for assisting with the preparation of otolith samples and members of the NOAA AFSC EcoFOCI field crews who collected larvae. We appreciate the helpful comments of three anonymous reviewer on an earlier version of this paper. The findings and conclusions in this paper are those of the authors and do not necessarily represent the views of the National Marine Fisheries Service. Reference to trade names does not imply endorsement by the National Marine Fisheries Service, NOAA. This paper is contribution EcoFOCI-1057 to NOAA's Ecosystems and Fisheries Oceanography Coordinated Investigations Program.

Author contributions

J. A. M.: Conceptualization; methodology; supervision; data collection; analysis; interpretation; writing – original draft, reviewing, and editing. L. Z. A.: Data collection; methodology; analysis; writing – reviewing. L. A. R.: Data collection and curation; interpretation; writing – reviewing. H. L. T.: Writing – reviewing. R. M. F.: Data collection; writing – reviewing. B. J. L.: Conceptualization; interpretation; writing – reviewing.

Funding
This work was supported by the North Pacific Research Board, Project No. 1903.

Competing interests
The authors declare no competing interests.

Additional information
Supplementary Information The online version contains supplementary material available at https://doi.org/10.1038/s41598-024-69915-1.

Correspondence and requests for materials should be addressed to J.A.M.

Reprints and permissions information is available at www.nature.com/reprints.

Publisher's note Springer Nature remains neutral with regard to jurisdictional claims in published maps and institutional affiliations.